Selective electron beam sensing through coherent Cherenkov diffraction radiation

E. Senes [ORCID], M. Krupa [ORCID], S. Mazzoni [ORCID], K. Lasocha [ORCID], T. Lefevre, A. Schloegelhofer [ORCID], and M. Wendt

CERN, CH-1211 Geneva 23, Switzerland

C. Davut [ORCID]

University of Manchester, Department of Physics and Astronomy, M13 9PL, Manchester, United Kingdom

P. Karataev [ORCID]

John Adams Institute at Royal Holloway, University of London, Egham, Surrey, TW20 0EX, United Kingdom

C. Pakuza and B. Spear

John Adams Institute at University of Oxford, University of Oxford, Oxford, OX1 3RH, United Kingdom

We exploit the coherent emission of Cherenkov diffraction radiation (ChDR) by a relativistic electron beam to sense its position even in the presence of other particle beams. ChDR is produced in alumina inserts embedded in the vacuum chamber walls and recorded in a narrow band centered at 30 GHz. This nontrivial solution has been implemented for plasma wakefield accelerators, where the electron beam to be sensed can copropagate with another high-energy proton beam that generates the plasma wakefield. In addition, at variance with most existing position detectors, this method is insensitive to spurious electric charges due to the presence of plasma. We present the overall design of the detector as well as experimental results obtained in the AWAKE facility at CERN.

I. INTRODUCTION

Particle accelerators are unique instruments driving interdisciplinary research including such disciplines as medicine [1], biology [2], chemistry [3], archaeology [4], and many other technical areas. Application in high energy physics has become a separate direction [5] requiring powerful acceleration technology alongside an extremely small emittance beam propagating over a multikilometer distance. A stable and reliable beam is required to achieve cutting edge and well reproducible results. Beam position monitors (BPM) are key noninvasive instruments at modern accelerator facilities enabling operators to maintain top beam quality [6]. They provide information about the beam position, direction, arrival time, charge, and tune, and demonstrate the beam stability. The need in beam position sensors has become obvious since the first accelerator was developed in 1929 [7]. A rather trivial phenomenon, e.g., interaction of electromagnetic field with metal structures, has resulted in a series of sophisticated designs including button sensors widely used in synchrotron light sources [8], strip line [9], and cavity [10] beam position monitors frequently used in linear accelerators. However, none of these designs are capable of distinguishing positions of two copropagating beams, i.e., beams propagating in the same direction in close temporal overlap.

AWAKE is a plasma-wakefield acceleration technology development project [11], where the wakefield is excited in a plasma channel by an intense 400 GeV proton beam, and then, a low intensity ultrashort electron beam is injected to gain the energy. For efficient acceleration, a precise control of the electron beam is needed in the presence of the more intense proton beam. In this paper we propose a beam position sensing technology. Cherenkov diffraction radiation (ChDR), appearing when a fast charge particle moves in the vicinity of a dielectric medium [12,13] is used to generate millimeter wave electromagnetic radiation in four dielectric rods placed around the beam trajectory. Coherent ChDR has already been applied for bunch length diagnostics in [14]. In our experiment the radiation propagating along the rod is measured by four sensitive detectors. The coherent part of the radiation spectrum was used to separate the signal between two copropagating beams of different lengths. Another significant advantage of this technology is that the ChDR is insensitive to superior charges from the plasma itself. Such a background limits the use of conventional BPM technologies.

This paper will present the conceptual description, analytical estimations, and electromagnetic simulations enabling to create a design used in the experimental test at AWAKE beam line. The experimental results and their analysis are presented and discussed.

II. SELECTIVE ELECTRON BEAM SENSING

A. Cherenkov diffraction radiation

A fast charged particle passing by a dielectric material polarizes atoms along its trajectory. The electron shells of

the polarized atoms then oscillate, emitting polarization radiation with a very broad spectrum propagating inside the medium. The mechanism is similar to classical Cherenkov radiation, however, the particle does not directly interact with the medium. Multiple scattering and bremsstrahlung processes do not affect the particle properties. On the other hand, finite outer dimensions of the radiator result in deviation of spectral-spatial properties of the emitted waves from classical Cherenkov radiation [13]. In [12] this phenomenon was assigned a new name of Cherenkov diffraction radiation (ChDR).

ChDR features very specific radiation characteristics that make it interesting for the noninvasive sensing of charged particle beams. The radiation is emitted at the characteristic Cherenkov angle θ_{Ch} [15] within the medium, according to

$$\cos(\theta_{Ch}) = \frac{1}{\beta n} \tag{1}$$

where $\beta = v/c$ is the speed of the particle in units of the speed of light in vacuum c, and n is the index of refraction of the medium. Recent advances in development of polarization radiation theory resulted in deriving a polarization current approach, which enabled us to develop models accounting for different radiation mechanisms such as transition radiation, diffraction radiation, Cherenkov diffraction radiation, and their interplay. In [13] the authors summarized the approach and made it suitable for estimating the spectral-spatial properties of ChDR from a single particle used as I_{SP} in Eq. (2) below.

B. Coherent radiation emission

The properties of the radiation emitted by a bunch of particles depend not only on the previously discussed single particle radiation properties, but also on the bunch structure. In [16] the authors assumed that synchrotron radiation can be emitted coherently, i.e., the intensity is proportional to the square of the number of particles within a bunch. Later it was theoretically and experimentally demonstrated that any mechanism might have coherent properties if the emission wavelength is comparable to or longer than the longitudinal size of the bunch. In this case, a phase relation exists among the single particles emitted radiation. The intensity of radiation emitted by a bunch of particles can be presented as [17,18]

$$I(\omega) = I_{SP}(\omega)[N + N(N-1)|f(\omega)|^2], \tag{2}$$

where I_{SP} is the single particle emission term (in this case, the ChDR emission term), ω is the angular frequency, N is the number of particles in the bunch, and $f(\omega)$ is the bunch form factor term. For sufficiently long wavelength, the emission from all the particles in the bunch can be assumed in phase, hence,

$$I_{Coh}(\omega) \propto N^2 I_{SP}(\omega)|f(\omega)|^2, \tag{3}$$

where $I_{Coh}(\omega)$ is the intensity of coherent radiation emitted by the bunch. For the purpose of selective beam sensing when multiple particle beams are present, the two key parameters are the particle population N and the longitudinal form factor, expressed by a Fourier transform of the longitudinal particle

distribution $\rho(z, \sigma_z)$ within the bunch. In the case of Gaussian longitudinal profile, the form factor can be represented as

$$f(\omega) = \int_{-\infty}^{\infty} \rho(z, \sigma_z) e^{-i\frac{\omega z}{c}} dz = e^{-\frac{\omega^2 \sigma_z^2}{2c^2}}. \tag{4}$$

Here z is the longitudinal coordinate and σ_z is the root-mean-square beam size of Gaussian distribution. In general, at low frequencies the impact of the bunch population dominates. At higher frequencies, the shape becomes the predominant factor. It is therefore possible to identify specific frequency regions of the spectrum where the radiation is dominated by the components from a single beam, even if it is not the most intense one. The specific application of this principle for the AWAKE beamline case is detailed in the Sec. II D.

C. Radiation field shaping

The radiation is produced at the surface of a dielectric radiator, which is parallel to the beam trajectory. The implementation in real accelerators poses physical constraints to the radiator shape and material, which reflects in a modification of the emitted radiation spectrum. The characteristics of the emitted radiation are affected by two key factors: radiator orientation and geometry.

First and foremost, internal reflections need to be controlled as much as possible. This is achieved by orienting the radiator at the Cherenkov angle θ_{Ch}. Second, ceramic cylindrical radiators are easy to manufacture and integrate with current technology. The confined propagation of the EM field in a dielectric radiator surrounded by the metal of the vacuum vessel, is analogous to that of a waveguide loaded with dielectric. For a cylindrical waveguide, the lowest order mode that can propagate features a low-cutoff frequency of

$$f_c = 1.8412 \frac{c}{2\pi r} \frac{1}{\sqrt{\epsilon_r}}, \tag{5}$$

where c is the speed of light, r is the radiator radius, and ϵ_r is the relative permittivity of the dielectric material [19]. Below the cutoff frequency, the fields are subject to an exponential damping along the radiator length [20].

The field generation and shaping is shown in Fig. 1. On the left, an engineering projection of the device is shown. The radiator is placed diagonally inclined exactly at the θ_{Ch}. The beam is passing by at a certain impact parameter (the shortest distance between the radiator and the particle trajectory, which is used for beam position sensing). On the right, the time evolution of the radiation production is shown from numerical simulations. The beam field is presented as a straight red line going from the beam to the radiator. The beam field is significantly more intense than the radiation field. It justifies the fact that the generation mechanism is nondestructive to the beam, because the energy loss due to the ChDR process is negligible. During the passage of the beam along the radiator edge, a wavefront is formed, and it propagates along the radiator at θ_{Ch} toward a detector. The radiation continues traveling slower than the particle beam at a speed of c/n, with $n = \sqrt{\epsilon_r \mu_r}$, where n is the refractive index of the medium, ϵ_r and μ_r are the relative permittivity and permeability of the radiator material. The radiation is finally refracted through the radiator exit face, where it can be detected. To minimize the radiation
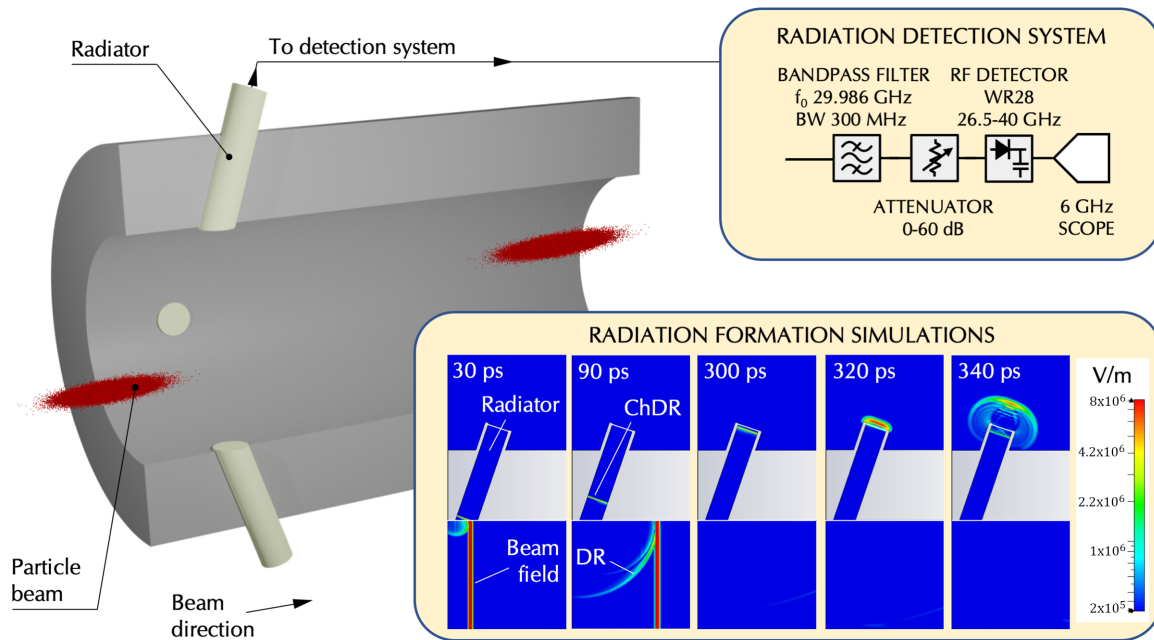
FIG. 1. On the left, the device schematic drawing including three ChDR pickups and two beams with an offset with respect to the chamber center. On the bottom right, a numerical simulation showing the temporal evolution of the electric field induced at the passage of the beam. The direct beam field, and the different radiation fronts, are indicated. The Cherenkov diffraction radiation front (ChDR) can be observed propagating throughout the radiator. The diffraction radiation (DR) production can be observed in the beampipe, as a result of the interaction of the beam field and the radiator edges. On the top right is the schematic diagram of the detection system.

distortion due to refraction, the exit face is made parallel to the incoming ChDR wavefront. One may see the diffraction radiation (DR) wavefront generated at the ChDR radiator and copropagating along the beam trajectory. The DR contribution is negligible with respect to the ChDR and can be ignored.

D. The radiator optimization

A prototype instrument was realized for the AWAKE experiment at CERN [11], where an intense proton "drive" beam is used to resonantly drive wakefields in a plasma, which are used to accelerate an electron "witness" beam. The aim of the instrument is to selectively sense the electron beam even in the presence of the proton beam, assuring the correct pointing before entering the plasma.

The characteristics of the two beams are largely different: the proton beam features the intensity of $1 - 3 \times 10^{11}$ particles per bunch, while the electron beam a charge of 100–600 pC ($0.6 - 3.8 \times 10^9$ particles per bunch). The bunch lengths (1σ) are also several orders of magnitude apart, with 250 ps for protons and a range between 1.5 and 5 ps for electrons. These differences have a strong impact on the spectrum of the coherent emission produced by the two beams. Assuming particle bunches of Gaussian shape, the different beam spectra calculated using Eqs. (3) and (4) are shown in Fig. 2. The spectra are normalized to the proton beam intensity. It can be noticed that although the emission spectrum is dominated by the intense proton beam at low frequency, its power quickly drops in the GHz range. Conversely, as the electron beam is shorter, its spectral power remains constant throughout a larger frequency range. It is therefore possible to select the electron emission with limited bias from the

protons, provided that the detection frequency is sufficiently high. For the purpose of this work, the target frequency for the electron beam detection was selected to be at 30 GHz, allowing for a large margin from the ideal proton emission drop frequency. This frequency choice was also selected to be sufficiently far from the plasma frequency, that in AWAKE exceeds 100 GHz [21]. This region is marked with the gray background in Fig. 2. In possible future application scenarios,
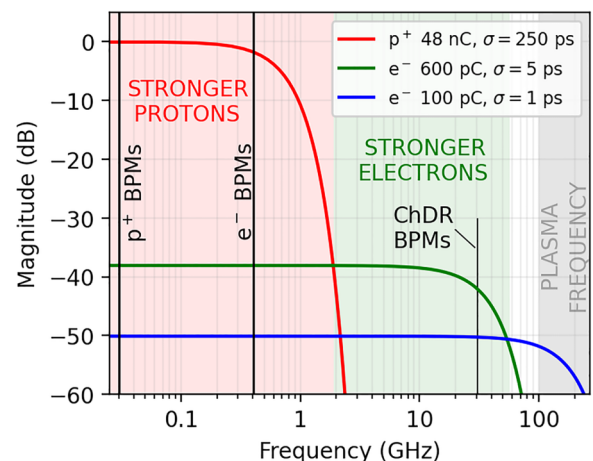

FIG. 2. Beam spectra for electron and proton beam for the AWAKE experiment. Gaussian bunch shapes are assumed. The vertical lines indicate the detection frequency of the different position sensors in the experiment. The spectra are dominated by the longitudinal bunch form factor $|f(\omega)|^2$.
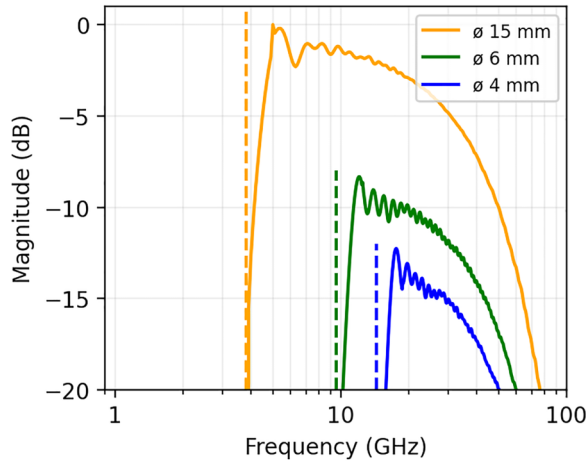
FIG. 3. Simulated relative power emission for different Al_2O_3 radiator diameters for a 600 pC, 4 ps-σ electron beam. The dashed lines indicate the theoretical cutoff frequency from Eq. (5).

FIG. 4. Signals for a 10^{11} proton beam, showing the depressed emission of the radiator below the noise level. When a 250 pC electron beam is added, it becomes clearly measurable even in the presence of the proton beam. For the case with both beams, the signal shown was attenuated of 10 dB.

the measurement might be performed in the presence of an in-plasma modulated proton beam.

The instrument was realized by brazing four opposite dielectric radiators in the vacuum vessel. The radiator material of choice was Alumina (Al_2O_3), which features the Cherenkov angle of 71° due to the high dielectric permittivity of 9.6 in the GHz range [22]. The large Cherenkov angle was selected to ease the mechanical integration within the existing accelerator.

The emission spectrum was designed not only to sense the electron beam at the 30 GHz frequency, but also to avoid producing large amounts of radiation from the protons below 1 GHz, which would have needed to be dissipated. To achieve this, cylindrical radiators were selected with a diameter of 6 mm, corresponding to a cutoff frequency of 9.6 GHz. The aperture of the beampipe is 60 mm. A study of the properties of the radiator emission was performed using a series of wakefield simulations in CST Studio Suite, produced by Dassault systèmes. The comparison of the normalized emitted power for different radiator diameters is shown in Fig. 3. The simulation results agree with the theoretical expectations of the low cutoff frequency, according to Eq. (5). At high frequency, the emitted power gradually decreases with frequency, as the incoherent regime is entered and the spectral power reduces. As the radiator dimension is reduced, the emitted power is also decreased, as the exposed face to be polarized by the beam becomes smaller.

III. EXPERIMENTAL SETUP

In this experiment, the radiation produced by each radiator is acquired and processed separately. The schematic of the radiation detection for a single radiator is presented in the top right of Fig. 1. This system is realized using standard WR28 waveguides, with a nominal TE10-mode operation frequency range of 26.5–40 GHz. The radiator output is channelled through a waveguide network 1.5 m long. Then, the radiation is filtered through a 30 GHz bandpass filter with a bandwidth of 300 MHz. A remotely controlled waveguide attenuator (MI-WAVE, model 511A) adapts the filtered signal
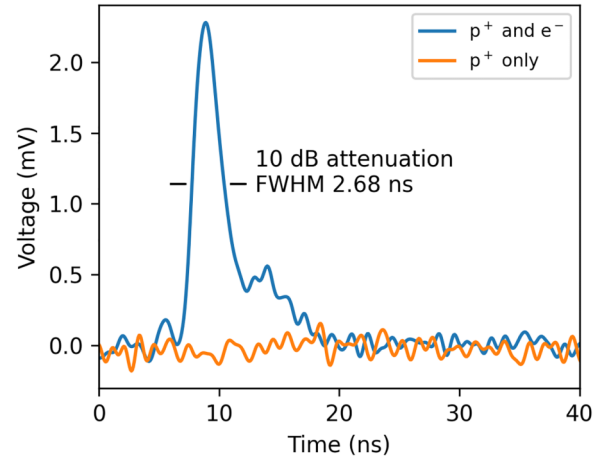
to the input of an RF detector. A zero-bias Schottky barrier diode detector (Millitech Inc., DXP-28) is used to rectify the filtered RF signal. The voltage at the coaxial output of the diode detector is then recorded by a 6 GHz oscilloscope (Tektronix, MSO6), and stored for further processing. During the experiment, the linear operation of the RF detector is obtained by limiting the input power with the attenuator. The input power on the detector is then reconstructed by knowing the attenuation setting for each measurement. The postprocessing enables extraction of the signal difference over sum for each beam position between two radiators in horizontal and vertical direction.

IV. RESULTS

The described device was tested with electron and proton beams in the AWAKE experiment. A good rejection of the proton signal components was measured. Figure 4 shows the comparison of the measured signal from the RF diode from one radiator for the proton beam alone and for electrons and protons. It is fundamental to note that the signal with electrons is attenuated of 10 dB. For a proton bunch of 1×10^{11} particles, the emitted power from the radiators is below the noise level of the available detection system. Conversely, the 250 pC electron bunch is clearly measurable even in presence of the more intense proton beam. The signal shape is conditioned by the RF detection chain shown in Fig. 1 (top right) and discussed in Sec. III. As the bandwidth of the filter is narrow (300 MHz in the 3 dB cutoff region), the resulting signal is stretched. The second shoulder, present after the main peak is to be attributed to the filter characteristic response, as confirmed by measurements with a vector network analyzer. The fast response of the radiators opens perspectives for realizing diagnostics for setups where multiple bunches are used. This was observed in the past [23], and will be the object of future studies. One may adjust the bandpass filter bandwidth versus the detector response; nevertheless, even the current setup can
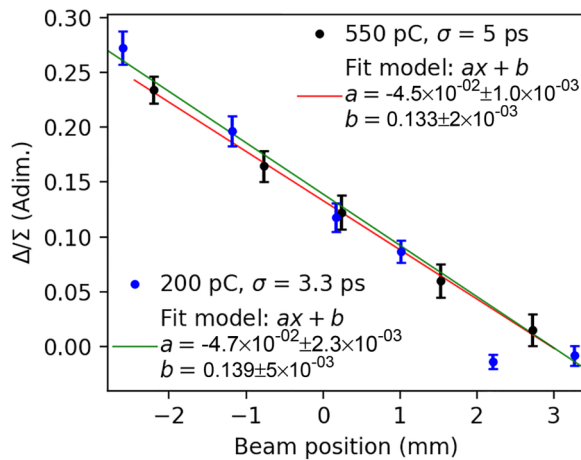
FIG. 5. Response for a position scan in the horizontal plane with a 200 and 550 pC electron beam. In the 200 pC data series, the point at the 2.2 mm position was excluded from the fit as a charge drift was detected.

resolve bunches, which are 2.68 ns apart (FWHM of the signal shown in Fig. 4).

A study with electron beam was performed to qualify the device response as a position monitor. The electron beam was displaced, and measured with an adjacent beam position monitor as reference. Both beams with 200 pC and 550 pC electrons per bunch were tested, exploring the extremes of the AWAKE beam parameter range. From reference measurements, these correspond to bunch lengths (1 σ) of 3.3 and 5 ps, respectively. The response to the beam position was estimated by calculating the difference over sum (Δ/Σ) of the amplitude of the RF voltage produced by two opposite radiator assemblies on the respective RF detectors. The measured response is showed in Fig. 5. The error bars indicate the standard deviation of the measurement in each position, calculated over an average of 200 acquisitions per data point. The contribution of the electron beam position jitter was subtracted. The response was found compatible with a linear fit in the explored 5 mm range. The measured sensitivity is $(4.7 \pm 0.2) \times 10^{-2}$ mm^{-1} for the 200 pC beam, and $(4.49 \pm 0.1) \times 10^{-2}$ mm^{-1} for the 550 pC beam. This has to be compared with the ideal sensitivity of 5.86×10^{-2} mm^{-1} from EM simulations. The electromagnetic center was not found around the center of the beampipe, but displaced of 3 mm due to the different radiator insertion losses. A number of causes contribute to the discrepancy between simulations and measurements, including the assumption of perfect symmetry, the idealized material properties, and response of the detection chain.

V. DISCUSSION

The integration of dielectric radiators is a substantial novelty in particle accelerators, where the field of position sensors has not had substantial conceptual improvement for decades. Furthermore, broadband detection of coherent radiation can be used to measure different beam parameters than position. For example, in [14] the authors have developed a technology

to reconstruct longitudinal electron beam profiles using three sensors detecting different spectral ranges. Replacing the detection system, one may diagnose the longitudinal profile.

The technology demonstrated in this work finds application in short bunch, high energy, charged particle accelerators. These parameters are increasingly common in state-of-the-art and future accelerators, that are progressively moving toward multi-GeV beam energies and sub-ps long bunches for both particle physics research [24,25] and x-ray production in free electron lasers (FELs) for base research [26]. For future accelerators relying on plasma technologies, the technique described in this work presents the additional advantage of being resilient to the free spurious charges present in the plasma environment. Plasma-accelerated beams typically present short bunch lengths due to the high plasma density used to obtain a strong acceleration [11], with demonstrated examples of schemes employing GeV-energy beams with sub-ps bunch lengths [27,28]. This is also the case for dielectric accelerators [29]. We have demonstrated 30 GHz beam position measurement technology. However, for shorter bunches (e.g., femtosecond duration) the technology can be extended to the detection of coherent radiation in the THz and optical range.

VI. CONCLUSIONS

We demonstrated that a beam induced radiation method can be applied for beam position sensing inside operational particle accelerators. This is a conceptually interesting approach to beam position diagnostics, enabling the discrimination of particle beams of different species based on bunch length. The use of dielectric materials enables placement of diagnostics in areas before impossible to reach, e.g., inside magnets and in plasma contaminated areas. Moreover, this approach allows the realization of monitors with a large bandwidth that exceeds tens of GHz, a regime difficult to access with conventional technologies with the current manufacturing capabilities.

This work showed that the selective sensing of an electron beam can be achieved even in the presence of a much more intense proton beam in close temporal and spatial proximity. This is realized by exploiting the very different beam parameters in combination with the use of radiative methods. The discrimination method exploiting the properties of the coherent radiation emission of the two beams was described. Experimental results with both electron and proton beams were shown, demonstrating the depression of the proton signal, and the sensitivity to the electron beam position.

The fast radiation emission is also promising for more complex beam arrangements, where multiple bunch trains are used.

[1] E. Engels, N. Li, J. Davis, J. Paino, M. Cameron, A. Dipuglia, S. Vogel, M. Valceski, A. Khochaiche, A. O'Keefe, M. Barnes, A. Cullen, A. Stevenson, S. Guatelli, A. Rosenfeld, M. Lerch, S. Corde, and M. Tehei, Toward personalized synchrotron microbeam radiation therapy, Sci. Rep. **10**, 8833 (2020).

[2] J. R. Helliwell, Synchrotron radiation facilities, Nat. Struct. Biol. **5**, 614 (1998).

[3] S. G. Wolf, L. Leiserowitz, M. Lahav, M. Deutsch, K. Kjaer, and J. Als-Nielsen, Elucidation of the two-dimensional structure of an α-amino acid surfactant monolayer on water using synchrotron x-ray diffraction, Nature (London) **328**, 63 (1987).

[4] M. Cherin, D. A. Iurino, M. Zanatta, V. Fernandez, A. Paciaroni, C. Petrillo, R. Rettori, and R. Sardella, Synchrotron radiation reveals the identity of the large felid from monte argentario (early Pleistocene, Italy), Sci. Rep. **8**, 8338 (2018).

[5] A. Wright and R. Webb, The large hadron collider, Nature (London) **448**, 269 (2007).

[6] M. Minty and F. Zimmermann, *Measurement and Control of Charged Particle Beams* (Springer Berlin, Heidelberg, 2003)

[7] A. Sessler and E. Wilson, *Engines of Discovery*, revised and expanded ed. (World Scientific, Singapore, 2014).

[8] Z. Chen, Y. Leng, K. Ye, G. Zhao, and R. Yuan, Beam position monitor design for a third generation light source, Phys. Rev. ST Accel. Beams **17**, 112801 (2014).

[9] R. J. Apsimon, D. R. Bett, N. Blaskovic Kraljevic, P. N. Burrows, G. B. Christian, C. I. Clarke, B. D. Constance, H. D. Khah, M. R. Davis, C. Perry, J. R. López, and C. J. Swinson, Design and performance of a high resolution, low latency stripline beam position monitor system, Phys. Rev. ST Accel. Beams **18**, 032803 (2015).

[10] Y. I. Kim, R. Ainsworth, A. Aryshev, S. T. Boogert, G. Boorman, J. Frisch, A. Heo, Y. Honda, W. H. Hwang, J. Y. Huang, E.-S. Kim, S. H. Kim, A. Lyapin, T. Naito, J. May, D. McCormick, R. E. Mellor, S. Molloy, J. Nelson, S. J. Park, Y. J. Park, M. Ross, S. Shin, C. Swinson, T. Smith, N. Terunuma, T. Tauchi, J. Urakawa, and G. R. White, Cavity beam position monitor system for the accelerator test facility 2, Phys. Rev. ST Accel. Beams **15**, 042801 (2012).

[11] E. Adli, A. Ahuja, O. Apsimon, R. Apsimon, A.-M. Bachmann, D. Barrientos, F. Batsch, J. Bauche, V. K. B. Olsen *et al.*, Acceleration of electrons in the plasma wakefield of a proton bunch, Nature (London) **561**, 363 (2018).

[12] R. Kieffer, L. Bartnik, M. Bergamaschi, V. V. Bleko, M. Billing, L. Bobb, J. Conway, M. Forster, P. Karataev, A. S. Konkov, R. O. Jones, T. Lefevre, J. S. Markova, S. Mazzoni, Y. Padilla Fuentes, A. P. Potylitsyn, J. Shanks, and S. Wang, Direct observation of incoherent cherenkov diffraction radiation in the visible range, Phys. Rev. Lett. **121**, 054802 (2018).

[13] M. V. Shevelev and A. S. Konkov, Peculiarities of the generation of vavilov-cherenkov radiation induced by a charged particle moving past a dielectric target, J. Exp. Theor. Phys. **118**, 501 (2014).

[14] A. Curcio, M. Bergamaschi, R. Corsini, W. Farabolini, D. Gamba, L. Garolfi, R. Kieffer, T. Lefevre, S. Mazzoni, K. Fedorov, J. Gardelle, A. Gilardi, P. Karataev, K. Lekomtsev, T. Pacey, Y. Saveliev, A. Potylitsyn, and E. Senes, Noninvasive bunch length measurements exploiting cherenkov diffraction radiation, Phys. Rev. Accel. Beams **23**, 022802 (2020).

[15] P. A. Čerenkov, Visible radiation produced by electrons moving in a medium with velocities exceeding that of light, Phys. Rev. **52**, 378 (1937).

[16] J. S. Nodvick and D. S. Saxon, Suppression of coherent radiation by electrons in a synchrotron, Phys. Rev. **96**, 180 (1954).

[17] G. P. Williams, C. J. Hirschmugl, E. M. Kneedler, P. Z. Takacs, M. Shleifer, Y. J. Chabal, and F. M. Hoffmann, Coherence effects in long-wavelength infrared synchrotron radiation emission, Phys. Rev. Lett. **62**, 261 (1989).

[18] M. Veronese, R. Appio, P. Craievich, and G. Penco, Absolute bunch length measurement using coherent diffraction radiation, Phys. Rev. Lett. **110**, 074802 (2013).

[19] J. D. Jackson, *Classical electrodynamics* (Wiley, New York, 1975).

[20] D. M. Pozar, *Microwave Engineering* (Wiley, New York, 2012).

[21] AWAKE Collaboration, Experimental observation of proton bunch modulation in a plasma at varying plasma densities, Phys. Rev. Lett. **122**, 054802 (2019).

[22] M. N. Afsar and K. J. Button, Precise millimeter-wave measurements of complex refractive index, complex dielectric permittivity and loss tangent of GaAs, Si, SiO_2, Al_2O_3, BeO, Macor, and Glass, IEEE Trans. Microwave Theory Tech. **31**, 217 (1983).

[23] E. Senes, Development of a beam position monitor for co-propagating electron and proton beams, Ph.D. thesis, 2020.

[24] A. Abada *et al.*, FCC-ee: The lepton collider, Eur. Phys. J. Spec. Top. **228**, 261 (2019).

[25] M. Aicheler, P. Burrows, M. Draper, T. Garvey, P. Lebrun, K. Peach, N. Phinney, H. Schmickler, D. Schulte, and N. Toge, *A Multi-TeV Linear Collider Based on CLIC Technology: CLIC Conceptual Design Report*, CERN Yellow Reports: Monographs (CERN, Geneva, 2012).

[26] C. Pellegrini, A. Marinelli, and S. Reiche, The physics of x-ray free-electron lasers, Rev. Mod. Phys. **88**, 015006 (2016).

[27] M. Litos *et al.*, High-efficiency acceleration of an electron beam in a plasma wakefield accelerator, Nature (London) **515**, 92 (2014).

[28] S. Schröder *et al.*, High-resolution sampling of beam-driven plasma wakefields, Nat. Commun. **11**, 5984 (2020).

[29] E. A. Peralta *et al.*, Demonstration of electron acceleration in a laser-driven dielectric microstructure, Nature (London) **503**, 91 (2013).

Correction: The name of the sixth author was misspelled and has been fixed.